WETLANDS, Vol. 27, No. 4, December 2007, pp. 1144–1152

MAPPING SALT MARSH VEGETATION USING AERIAL HYPERSPECTRAL IMAGERY AND LINEAR UNMIXING IN HUMBOLDT BAY, CALIFORNIA

Chaeli Judd[1,4], Steven Steinberg[1], Frank Shaughnessy[2], and Greg Crawford[3]
[1]*Department of Environmental and Natural Resources*

[2]*Department of Biological Sciences*

[3]*Department of Oceanography*
Humboldt State University
Arcata, California, USA 95521

[4]*Present address*
Pacific Northwest National Laboratory, Marine Sciences Operation
Sequim, Washington, USA 98382
E-mail: chaeli.judd@pnl.gov

Abstract: Composition of salt marsh vegetation is important to wetland ecosystem health, and monitoring invasive species is critical. The purpose of this study was to examine the utility of airborne hyperspectral imagery in mapping salt marsh vegetation in Humboldt Bay, California, USA. An unmixing algorithm was applied to spatial and spectral image subsets. Overall accuracy among *Spartina densiflora*, *Salicornia virginica*, and *Distichlis spicata* was assessed at 85.1%. Algorithm prediction between observed and predicted percent cover ranged from $r^2 = 0.32$ to $r^2 = 0.53$, an improvement on comparable studies. Percent cover prediction was least accurate for *Distichlis spicata*, due to initial endmember selection. Use of the Pixel Purity Index in conjunction with field work likely aided in identifying the best candidates for the linear unmixing technique.

Key Words: Pacific Northwest, remote sensing, *Spartina*, wetlands

INTRODUCTION

Over the past 200 years, coastal wetlands in the United States have undergone significant changes in spatial extent (Dahl 1990, Dahl 2006) and species composition (Thompson 1991, Galatowitsch et al. 1999). Today, expanding urban areas as well as the introduction and propagation of exotic species are changing the face of many coastal salt marshes. From a management perspective, having information not only about the spatial distribution but also species composition in salt marsh habitats is critical. Most existing maps that describe estuarine habitat types do not provide that level of detail. The National Wetlands Inventory, for example, uses broad habitat classes to describe characteristics of wetlands (Cowardin et al. 1979). Additional wetlands map information, such as species distribution, is not generally available and requires intensive site-specific field work methods (USACE 1987).

In the Pacific Northwest, documenting and monitoring the distribution of *Spartina* species is of particular concern. Many types of cordgrass species are invasive, growing in the intertidal/upper intertidal zones of estuaries in thick monospecific stands. Because of its dense structure, *Spartina* has the potential to outcompete native salt marsh vegetation, altering the dynamics of salt marsh ecosystems. Invasive cordgrass is expanding and has the potential to spread quickly to unaffected areas (Daehler and Strong 1996, Clifford 2002). However, current methods for monitoring *Spartina* rely on intensive field work (Pickart 2001, Collins et al. 2002).

Recent advances in airborne hyperspectral sensor technologies enable more complete and accurate classification of wetlands, including species specific mapping (Alberotanza 1999, Okin et al. 2001, Hirano et al. 2003). Hyperspectral imagery contains many more bands of information than what a traditional air photo provides. While the bands are in the same wavelength ranges as traditional true color or color infrared images, each individual band is narrower in spectral width. Therefore, the bands can be viewed together as an approximation of a spectral curve (see Figure 1). In addition, specific chemical properties,

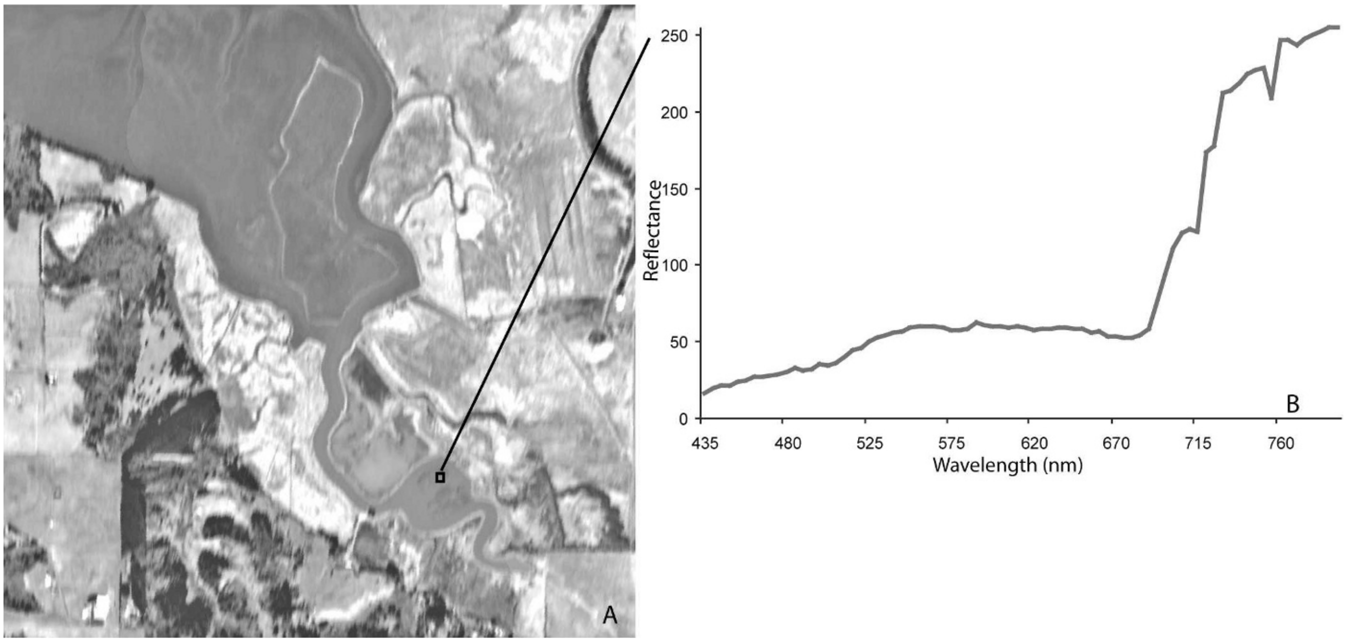

Figure 1. Spectral curves from hyperspectral imagery. Since every pixel in the image (A) contains 122 contiguous bands, the bands can be viewed together as an approximation of a spectral curve. In this case, the pixel identified represents a 4 m $\times$ 4 m area in the salt marsh covered by *Salicornia virginica* in South Humboldt Bay. The spectral response is typical of *S. virginica*, with an increase in reflectance in the infrared range (B).

such as absorption in a certain wavelength, may be targeted. Studies using readings from field spectrometers have shown promise in separation of vegetation species by their spectral curves (Schmidt and Skidmore 2003, Artigas and Yang 2006).

In recent years, a variety of algorithms have been developed to classify hyperspectral imagery (Boardman 1989, Kruse et al. 1993, Boardman et al. 1995). After atmospheric correction, a library of reference spectral curves (known as spectral endmembers), either of an individual's creation or a standard database, can be referenced to define the species present in an unknown spectrally pure pixel (i.e., a pixel of homogenous cover). Even non pure pixels can be dissected mathematically to discern which components of the spectral library and what proportion of those endmembers are represented in a specific area. The reality is a bit more complex. Any one species or target can have a variety of spectral responses depending on season, water content, and physiological condition (Gates et al. 1965, Carter and Knapp 2001). In addition, more often than not, a pixel is not spectrally pure. A variety of elements, such as soil, water, detritus, and canopy leaves may occur in a pixel. Because of this variance, it is difficult to find truly pure pixels. There have been inconsistencies when using a manually created spectral library to match canopy reflectance in hyperspectral image mapping of salt marsh vegetation (Sauer 2006).

The pixel purity index (PPI), developed by Boardman et al. (1995), is an automated process that identifies pixels in an image that are statistically extreme and considered to represent the purest spectral endmembers. Because the algorithm identifies statistically "pure" pixels without user prejudice, many analyses of canopy level classifications in vegetation have relied on the use of the PPI.

While the use of hyperspectral imagery may provide more information and better classification, few published studies have actually produced hyperspectral mapping results for salt marsh vegetation. The goal of this study was to assess the utility of airborne hyperspectral image analysis in mapping dominant salt marsh vegetation type, association, and percent cover by using PPI results to select endmembers.

METHODS

Study Area

Humboldt Bay, located on the coast of northern California, is comprised of three bays, the largest of which is Arcata Bay. Twenty-two known plant species are found in the salt marsh with three described associations: *Salicornia virginica*, *Spartina densiflora*, and mixed marsh (Eicher 1987, Pickart 2006). *Salicornia virginica*, *Spartina densiflora*, and *Distichlis spicata* make up more than 80% of the

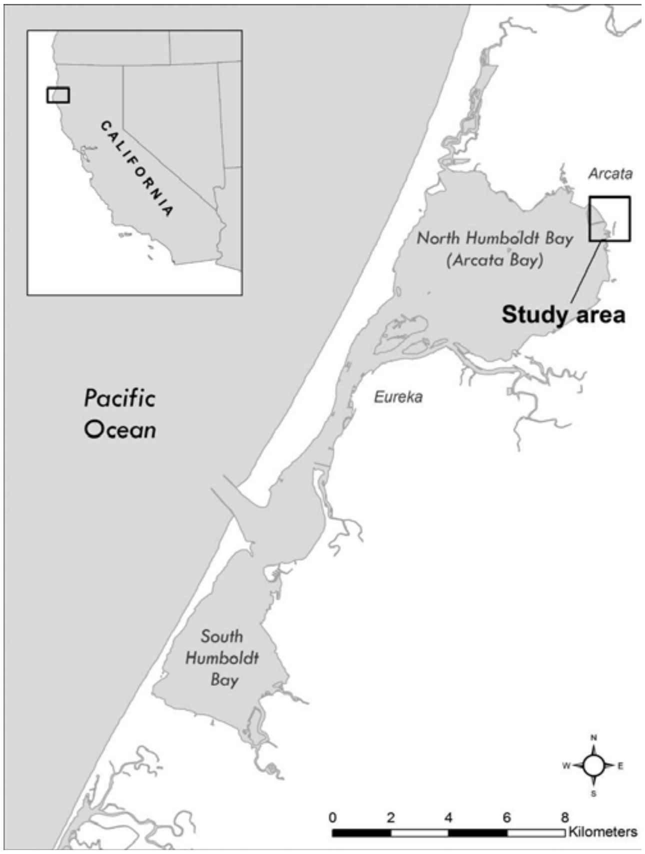

Figure 2. Study Area. The study area located in Humboldt Bay in Northern California.

plant cover in previously studied areas (Eicher 1987). Our study site was located in Arcata Marsh, on the northeastern edge of Arcata Bay (Figure 2) and contained 13 ha of salt marsh (Figure 3). Elevation within the study area ranges from roughly +2.13 m to +2.74 m relative to mean lower low water (MLLW).

Data Sources

Hyperspectral imagery was collected in October 2004 using a Navy Research Laboratory Portable Hyperspectral Imager for Low Light Spectroscopy II (PHILLS II) sensor (Davis et al. 2002). As part of a multi-goal project to characterize both emerged and submerged vegetation, October was chosen because plant biomass is still high and water clarity is at its best. The resulting image contained 122 bands ranging from blue (421 nm) to near infrared wavelengths (966 nm), with a bandwidth of 4.5 nm. The flight and preprocessing were carried out by Florida Environmental Research Institute (FERI). Atmospheric correction was completed using a modified TAFKAA model with spectral matching to standard atmospheric values as described by Gao et al. (2004). Pixels were 4 m $\times$ 4 m. However, due to an underestimate of the instantaneous field of view (IFOV), there was an overlap of information in the pixels. The actual pixels contain 4 m $\times$ 12 m worth of information, indicating a 3 pixel overlap in the along track direction. Due to noise, a total of 44 bands were eliminated on both ends of the spectrum. Seventy-eight remaining contiguous bands (435–794 nm) were used in this analysis. Average tidal height was +2.13 m at the time of data acquisition (North Spit, California, USA tidal station).

Topographic LIDAR data (Figure 4), collected in 2002 at an extreme low tide, was used to estimate elevation. Data were adjusted to MLLW using a linear weighting method from known tidal benchmarks. Ground truth points for dominant cover were collected in transects from February to April, 2006, using a Garmin GPS device (GPS 76, Garmin International, Inc., Olathe, Kansas, USA). Ground

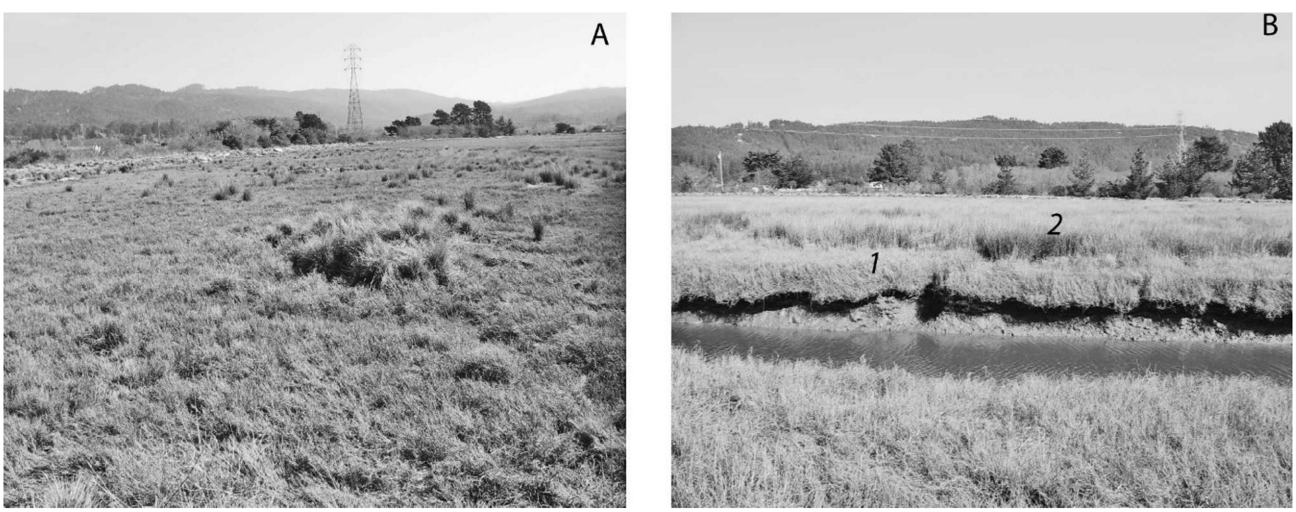

Figure 3. Photos show a *Distichlis spicata* alliance (A) where *D. spicata*, although dominant, is interspersed with tufts of *S. densiflora* and *S. virginica*, and a *Salicornia virginica* (B-1) alliance area bordering on a *Spartina densiflora* alliance (B-2).

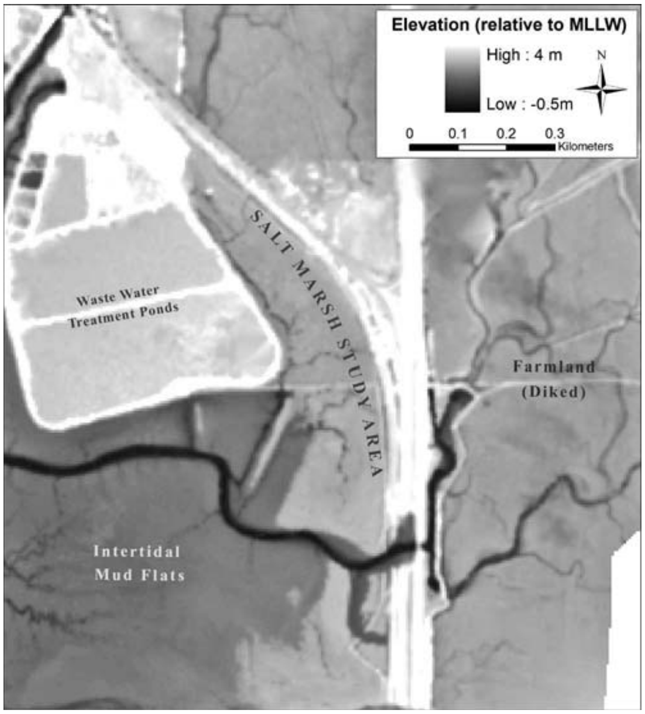

Figure 4. Elevation of area. LIDAR image shows elevation difference in salt marsh study area versus surrounding mudflats, structures, and channels. A breached dike running through study area permits tidal flow in the northern portion while the southern portion is not diked.

truth points for percent cover were collected in April 2006 using a differentially correctable Trimble GPS (GeoXT, Trimble Navigation, Ltd., Sunnyvale, California, USA). Root mean square error at the time of data collection was up to $\pm$ 5 m for the Garmin, and $<$ 1 m for the Trimble. Because of this error and data blurring, attempts were made to collect data points in the middle of each target.

Data Analysis

Using the LIDAR dataset, a hyperspectral image subset was produced by using an elevation mask to only include areas that could be salt marshes between +1.83 m and +2.75 m relative to MLLW (Eicher 1987). The subset area was transformed using an inverse minimum noise fraction transformation, as described by Green et al. (1998).

A purity pixel index (PPI) was calculated for the image subset using the Environment for Visualizing Image*s* software (ENVI 4.3, RSI, Boulder, Colorado, USA). Areas of contiguous pixels that were calculated to be "spectrally pure" were selected to be ground truthed. In the field, areas that represented areas of near homogenous vegetation cover and were identified as spectrally pure pixels were marked with a GPS unit, including areas for *Spartina*, *Salicornia*, *Distichlis*, mud, and water.

In ENVI, regions of interest (polygons) were drawn around the selected ground truthed areas as identified in the previous step. One or two regions of interest were defined for each vegetation target of interest. Using a linear unmixing algorithm, as developed by Kruse et al. (1993), the spectral means of the regions of interest were used as spectral endmembers, and the classification was calculated.

Accuracy Assessment

Trimble GPS points were differentially corrected and saved in ESRI shapefile format. The Garmin points were also saved. Both were imported into ArcGIS (ArcGIS 9.1, Environmental Systems Research Institute, Inc., Redlands, California, USA), and these reference points were compared with the classification. An error matrix was produced for percent cover using the Trimble points as well as dominant species, using both sources.

RESULTS AND DISCUSSION

A map of vegetation dominance/alliance type for Arcata Marsh was produced (Figure 5). In total, 4.7 ha of *Spartina*, 5.0 ha of *Distichlis*, and 3.4 ha of *Salicornia* marsh were mapped over the 13.2 ha study area. Classification accuracy was estimated at 85.1% between *Spartina* dominant, *Salicornia* dominant, and *Distichlis* coverages, with a Kappa coefficient of 0.762 (Table 1). Producer's accuracy, which calculates how much of a ground vegetation type was correctly classified as that species (error of omission), had the highest accuracy for *Spartina* and *Salicornia*. However, *Spartina* tended to be overclassified in the ground truthed areas. User's accuracy, which looks at how well a classification matches that class on the ground (error of commission), had the lowest accuracy for *Spartina*, due to confusion with *Distichlis*.

Results from the linear unmixing algorithm are shown in Figure 6. Given the error in the previous map, classification results showed a good correlation with the field observed coverage at the sample points. It was particularly encouraging to note that large monotypic stands of *S. densiflora* observed on the ground had been classified as having from 80%–100% coverage. The RMS error image was without obvious pattern within the interior of the salt marsh. However, error was high in pixels on the outer boundary of the study area. It was likely that as the vegetation changed between habitats, the endmem-

Table 1. Classification accuracy for hyperspectral salt marsh mapping. This includes a comparison of actual dominant species gathered from ground truth to the mapped dominant species as classified by the analysis as well as user's and producer's accuracy.

Classified Dominant Species (from map)	Actual Dominant Species (from field work) *Spartina densiflora*	*Salicornia virginica*	*Distichlis spicata*	Total	Error of commission	User's Accuracy
Spartina densiflora	13	2	4	19	31.6%	68.4%
Salicornia virginica	0	25	5	30	16.7%	83.3%
Distichlis spicata	1	1	36	38	5.3%	94.7%
Total	14	28	45	87		
Error of omission	7.1%	10.7%	20.0%			
Producer's Accuracy	92.9%	89.3%	80.0%			85.1%

bers were less representative of the ground cover truly found in the region.

Use of a Pixel Purity Index to Choose Endmembers

Compared to similar salt marsh mapping studies with hyperspectral data (Rosso 2005, Sauer 2006), this mapping project had a high accuracy rate. It is probable that the use of the PPI and field work to select statistically pure areas aided in identifying the best candidates for the linear unmixing algorithm. In direct contrast, Rosso et al. (2005) found better results from models that used field selected endmembers over PPI selected endmembers. However, by field checking areas that were calculated by the PPI to be the purest, we were able to integrate the best of both methods: selecting statistically extreme areas that on the ground were monotypic. Since the linear unmixing technique depends on image based values rather than real world spectral responses, the extreme image pixels would create a more viable equation than a field based value. Nevertheless, the differences in vegetation type or cover do not account for the all of the variance in reflectance values. While limiting the analysis to known and desired end mapping features probably resulted in a higher average RMSE, the end mapping result corresponded better with our objective than using unknown extreme endmembers.

Figure 5. Hyperspectral marsh vegetation classification. Accuracy was assessed at 85.1% for marsh vegetation.

In predicting the percent coverage, there was a relatively good correlation between predicted and observed percent coverages for both *S. densiflora* and *S. virginica*, but *D. spicata* had a lower correlation (Figure 7). This is probably due to the initial endmember selection. Although the image was taken in October, when plant biomass was high, the actual field work was carried out from January to April, when the above ground *Salicornia*, *Distichlis*, and *Spartina* were physically present, but dormant. The extent of the rhizome dormant arrowgrass (*Triglochin maritima*) was not observed until April. Co-occurring with *D. spicata* and *S. virginica*, *T. maritima* coverage ranged from 0%–30% in the April ground truth sites, but appeared to be higher in other areas. This was not sufficient to be a dominant coverage, but likely did affect endmember selection for *Distichlis*. In June, the areas selected in the endmember selection were revisited on the ground. One of the two *Distichlis* areas

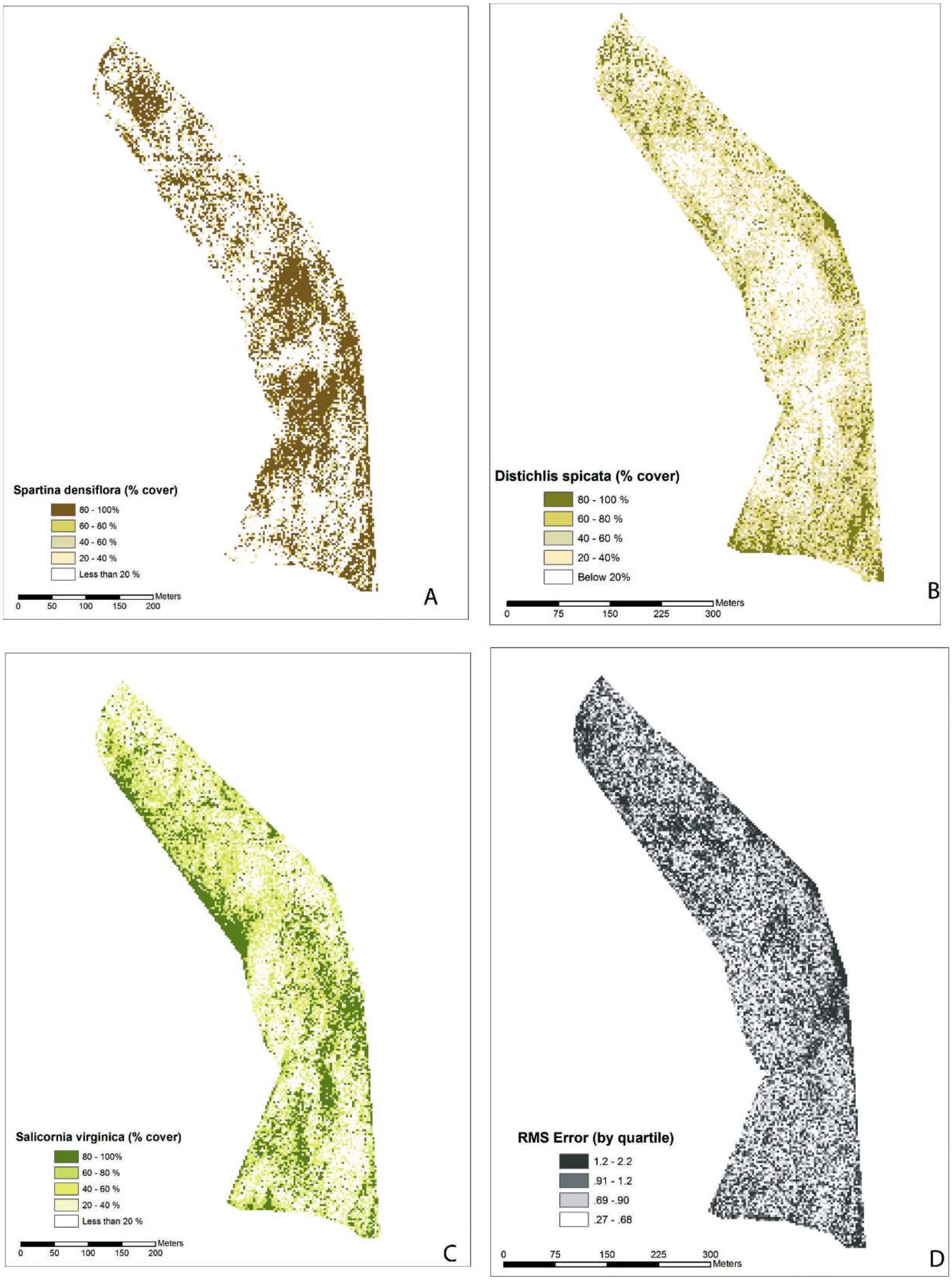

Figure 6. Linear unmixing results by dominant species from hyperspectral imagery. *Spartina densiflora* (A) and *Salicornia virginica* (C) have a greater correlation with actual cover than *Distichlis spicata* (B).

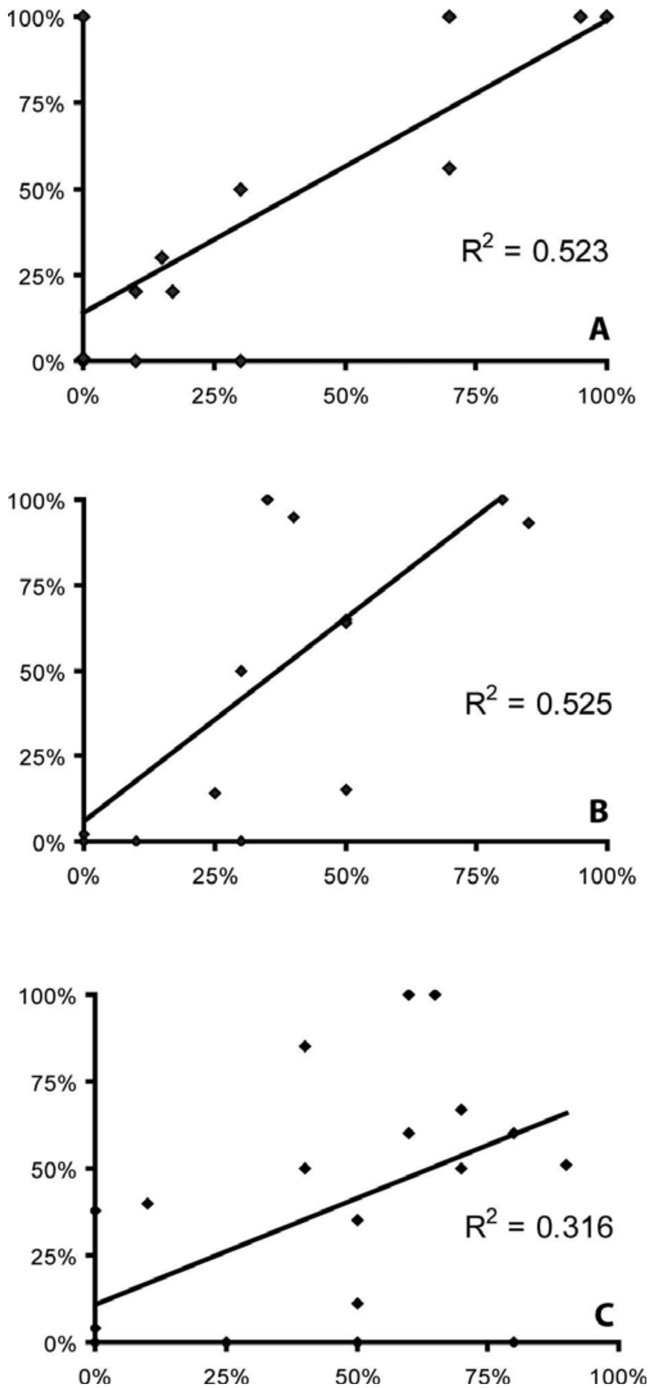

Figure 7. Relation between observed and predicted vegetation coverage for A) *Spartina densiflora*, B) *Salicornia virginica*, and C) *Distichlis spicata*.

showed an estimated 35% coverage of *T. maritima* (Figure 8). The mean spectral curve used for the linear unmixing algorithm was not a pure sample of *D. spicata* as was initially believed. Areas that rated highest in the linear unmixing for this sample were actually a mixture of *D. spicata* and *T. maritima*. This led to some of the classification problems with *Distichlis* and probably accounts for the lower correlation between predicted and observed coverage for *Distichlis* than for *Salicornia* and *Spartina*. If field work had been carried out in the same season as data acquisition, this problem could have been avoided. Additional increases in discrimination potential may be reached through image acquisition during the summer season.

Mapping Dominant Vegetation versus Mapping Vegetation Alliance

Mapping dominant vegetation in a pixel is inherently difficult when several species occupy the same area on the ground. In this classification, some error can be attributed to various amounts of the target marsh species occurring in each pixel. While a pixel may be classified as one of the species present, it may not necessarily be the dominant one. This is particularly true of the high marsh areas where *D. spicata* and *S. virginica* co-occur. Mapping on the alliance level instead of the species level would increase classification accuracy. Including an alliance of *Distichlis spicata* - *Salicornia virginica*, for example, would eliminate the need to estimate dominance in a pixel where both are present. Mapping on a pixel level also presents difficulties when variance takes place at a subpixel level. For example, *S. virginica* and *S. densiflora* are spatially located near one another, but usually are separated by very abrupt zonation transitions and spectrally are very different. Misclassification between *Salicornia* and *Spartina* only occurred when both species were present in the same area on the ground. Using a higher resolution image would likely increase classification accuracy in this case.

CONCLUSION

Hyperspectral imagery can be used to successfully map salt marsh species where *D. spicata*, *S. virginica*, and *S. densiflora* are the principal vegetation species. The integration of LIDAR elevation data helps to limit the study area to known elevations of salt marsh habitat. While there was a good correlation between predicted and observed percent cover for dominant vegetation species, the linear unmixing algorithm is not foolproof. Both user error in endmember selection and spectral variance within the target vegetation species prevented higher correlations. However, the unmixing algorithm did a good job in mapping spatially the highest density of each class. In particular, dense *Spartina* was correctly mapped. It is probable that mapping on an alliance level would increase result accuracy.

Figure 8. Endmember selection area in June. *Triclochin* (Tr) is found among the *Distichlis* (Di).

ACKNOWLEDGMENTS

This study was made possible through invaluable field support and local knowledge of Jennifer Kauffman and Milton Boyd from Humboldt State University, Andrea Pickart from the USFWS, and the late Jeff Robinson from Humboldt Bay Harbor and Conservation District. Florida Environmental Research Institute provided technical assistance. Research was funded by NOAA (Award NA16OC2907) as part of the Center for Integrative Coastal Observation, Research, and Education (CICORE) on-going research activities.

LITERATURE CITED

Alberotanza, L. 1999. Hyperspectral aerial images: a valuable tool for submerged vegetation recognition in the Orbetello Lagoons, Italy. International Journal of Remote Sensing 20:523–33.

Artigas, F. and J. Yang. 2006. Spectral discrimination of marsh vegetation types in the New Jersey Meadowlands, USA. Wetlands 26:271–77.

Boardman, J. W. 1989. Inversion of imaging spectrometry data using singular value decomposition. Geoscience and Remote Sensing Symposium, IGARSS'89, 12th Canadian Symposium on Remote Sensing 4:2069–72.

Boardman, J. W., F. A. Kruse, and R. O. Green. 1995. Mapping target signatures via partial unmixing of AVIRIS data. *In* R. O. Green (ed.) Summaries, Fifth JPL Airborne Earth Science Workshop, JPL Publication 95–1, 1: 23–26.

Carter, G. and A. Knapp. 2001. Leaf optical properties in higher plants: linking spectral characteristics to stress and chlorophyll concentration. American Journal of Botany 88:677–84.

Clifford, P. 2002. Dense-flowered cordgrass (*Spartina densiflora*) in Humboldt Bay, Summary and Literature Review. California State Coastal Conservancy Report, Oakland, CA, USA.

Collins, J., M. May, D. Smith, S. Klohr, and K. Zaremba. 2002. Data Collection Protocol. Distribution, Abundance, and Treatment of Non-indigenous Species of Cordgrass in the San Francisco Estuary. Wetlands Regional Monitoring Program Plan 2002, Report for California Coastal Conservancy, Oakland, CA, USA.

Cowardin, L., V. Carter, F. Golet, and E. LaRoe. 1979. Classification of wetlands and deepwater habitats of the United States. US Department of the Interior, Fish and Wildlife Service, FWS/OBS–79/31.

Daehler, C. and D. Strong. 1996. Status, prediction and prevention of introduced cordgrass *Spartina* spp. invasions in Pacific estuaries, USA. Biological Conservation 78:51–58.

Dahl, T. E. 1990. Wetlands losses in the United States 1780s to 1980s. U.S. Department of the Interior, Fish and Wildlife Service, Washington, DC, USA.

Dahl, T. E. 2006. Status and trends of wetlands in the conterminous United States 1998 to 2004. U.S. Department of the Interior, Fish and Wildlife Service, Washington, DC, USA.

Davis, C., J. Bowles, R. Leathers, D. Korwan, V. Downes, W. Snyder, W. Rhea, W. Chen, J. Fisher, P. Bissett, and R. Reisse. 2002. Ocean PHILLS hyperspectral imager: design, characterization and calibration. Optic Express 10:210–21.

Eicher, A. 1987. Salt marsh vascular plant distribution in relation to tidal elevation, Humboldt Bay, California. M.S. Thesis. Humboldt State University, Arcata, CA, USA.

Galatowitsch, S., N. Anderson, and P. Ascher. 1999. Invasiveness in wetlands plants in temperate North America. Wetlands 19:733–55.

Gao, B., M. Montes, and C. Davis. 2004. Refinement of wavelength calibrations of hyperspectral imaging data using a spectrum-matching technique. Remote Sensing of Environment 90:424–33.

Gates, D., H. Keegan, J. Schleter, and V. Weidner. 1965. Spectral properties of plants. Applied Optics 4:11–20.

Green, A., M. Berman, P. Switzer, and M. Craig. 1988. A transformation for ordering multispectral data in terms of image quality with implications for noise removal. IEEE Transactions on Geoscience and Remote Sensing 26:65–74.

Hirano, A., M. Madden, and R. Welch. 2003. Hyperspectral image data for mapping wetland vegetation. Wetlands 23:436–48.

Kruse, F. A., A. B. Lefkoff, J. B. Boardman, K. B. Heidebrecht, A. T. Shapiro, P. J. Barloon, and A. F. H. Goetz. 1993. The Spectral Image Processing System (SIPS) - interactive visualization and analysis of imaging spectrometer data. Remote Sensing of Environment 44:145–63.

Okin, G., D. Roberts, B. Murray, and W. Okin. 2001. Practical limits on hyperspectral vegetation discrimination environments. Remote Sensing of Environment 77:212–25.

Pickart, A. 2001. The distribution of *Spartina densiflora* and two rare salt marsh plants in Humboldt Bay 1998–1999. USFWS Unpublished Report.

Pickart, A. 2006. Vegetation of diked herbaceous wetlands of Humboldt Bay National Wildlife Refuge: classification, description and ecology. Draft USFWS Report.

Rosso, R., S. Ustin, and A. Hastings. 2005. Mapping marshland vegetation of San Francisco Bay, California, using hyperspectral data. International Journal of Remote Sensing 26:5169–91.

Sauer, M. 2006. Airborne hyperspectral remote sensing of salt marsh vegetation in Moro Bay, California. M.S. Thesis. California State University, San Luis Obispo, CA, USA.

Schmidt, K. and A. Skidmore. 2003. Spectral discrimination of vegetation types in a coastal wetland. Remote Sensing of Environment 85:92–108.

Thompson, J. 1991. The biology of an invasive plant. BioScience 41:393–401.

USACE. 1987. Corps of engineers wetlands delineation manual. U.S. Army Corps of Engineers, Waterways Experiment Station, Vicksburg, MS, USA. Y–87–1.

Manuscript received 20 June 2006; accepted 20 August 2007.